ELSEVIER

NeuroImage

www.elsevier.com/locate/ynimg
NeuroImage 25 (2005) 746–755

Unified SPM–ICA for fMRI analysis

Dewen Hu,[a,b,*] Lirong Yan,[a] Yadong Liu,[a] Zongtan Zhou,[a] Karl J. Friston,[c] Changlian Tan,[d] and Daxing Wu[e]

[a]*College of Mechatronics and Automation, National University of Defense Technology, Changsha, Hunan 410073, PR China*
[b]*Key Laboratory of Mental Health, Institute of Psychology, Chinese Academy of Sciences, Beijing 100101, PR China*
[c]*Wellcome Department of Imaging Neuroscience, Institute of Neurology, 12 Queen Square, London WC1N 3BG, UK*
[d]*Department of Radiology, the Second Xiangya Hospital of Center South University, Changsha 410011, PR China*
[e]*Research Center of Psychology, the Second Xiangya Hospital of Center South University, Changsha 410011, PR China*

Received 22 April 2004; revised 4 November 2004; accepted 14 December 2004
Available online 17 February 2005

A widely used tool for functional magnetic resonance imaging (fMRI) data analysis, statistical parametric mapping (SPM), is based on the general linear model (GLM). SPM therefore requires a priori knowledge or specific assumptions about the time courses contributing to signal changes. In contradistinction, independent component analysis (ICA) is a data-driven method based on the assumption that the causes of responses are statistically independent. Here we describe a unified method, which combines ICA, temporal ICA (tICA), and SPM for analyzing fMRI data. tICA was applied to fMRI datasets to disclose independent components, whose number was determined by the Bayesian information criterion (BIC). The resulting components were used to construct the design matrix of a GLM. Parameters were estimated and regionally-specific statistical inferences were made about activations in the usual way. The sensitivity and specificity were evaluated using Monte Carlo simulations. The receiver operating characteristic (ROC) curves indicated that the unified SPM–ICA method had a better performance. Moreover, SPM–ICA was applied to fMRI datasets from twelve normal subjects performing left and right hand movements. The areas identified corresponded to motor (premotor, sensorimotor areas and SMA) areas and were consistently task related. Part of the frontal lobe, parietal cortex, and cingulate gyrus also showed transiently task-related responses. The unified method requires less supervision than the conventional SPM and enables classical inference about the expression of independent components. Our results also suggest that the method has a higher sensitivity than SPM analyses.

Keywords: Independent component analysis (ICA); Statistical parametric mapping (SPM); Functional MRI; Brain activation; Motor paradigm; Consistently task-related responses; Transiently task-related responses

Introduction

Statistical parametric mapping (SPM), based on the general linear model (GLM), is a powerful tool for the analysis of functional mapping experiments (Friston et al., 1994, 1995a,b). To measure the magnitude of the blood-oxygenation-level-dependent (BOLD) signal that is task-specific, neuroimaging data at each voxel are modeled as a linear combination of explanatory variables plus a residual error term (Friston et al., 1995c). SPM creates images of a statistic reflecting 'significance'. These SPMs are interpreted as spatially extended statistical processes that behave according to the theory of Gaussian fields (Adler, 1981). This enables the statistical characterization of regionally specific responses (e.g., using t tests or F tests). This technique makes it possible to test multiple factors that may contribute to the signal changes in neuroimaging data.

SPM, by its nature, is model-driven and depends on some hypotheses about the data. These hypotheses are embodied in the design matrix of the GLM. Furthermore, it is a univariate approach, because it characterizes each voxel separately and performs voxel-wise statistical analyses in parallel. The application of the GLM proceeds under two assumptions: normal distribution and independence of the error terms. In neuroimaging, several factors can change the observed data. Some are related to the BOLD signal changes evoked by specific tasks and experimental conditions, and some represent noise, originating from physiological effects (e.g., cardiac and respiratory effects) or measurements (e.g., thermal noise or noise due to head movement).

SPM offers several options to model evoked changes in signal intensities (Della-Maggiore et al., 2002), including a canonical hemodynamic response function (HRF), which can be supplemented with various derivatives. For example, a temporal derivative that models slight onset differences. These basis functions are used to create regressors in the design matrix. The ensuing GLM is a convolution model that depends on knowing the form of the HRF. However, assumptions about the HRF are not

* Corresponding author. College of Mechatronics and Automation, National University of Defense Technology, Changsha, Hunan 410073, PR China. Fax: +86 731 4574992.
E-mail address: dwhu@nudt.edu.cn (D. Hu).
Available online on ScienceDirect (www.sciencedirect.com).

1053-8119/$ - see front matter © 2004 Elsevier Inc. All rights reserved.
doi:10.1016/j.neuroimage.2004.12.031

always valid. For example, some voxels may show an 'initial dip' whereas others may not (Grinvald et al., 2000; Lindauer et al., 2001; Mayhew, 2003; Mayhew et al., 1998, 1999, 2001; Thompson et al., 2003), and different stimuli may elicit different kinds of hemodynamic responses (Friston et al., 1998). If the assumed forms of the HRF, or the stimulus functions it is convolved with, are incorrect or incomplete, this may result in biased estimates of the true response (Fadili et al., 2000).

Complementary methods, driven by the data, do not make any assumption about the causes of responses or the form of the HRF. They have been applied to functional mapping experiments in the context of principal component analysis (PCA) (Backfrieder, 1996), Blind source separation (BSS) (Stone, 2001), and clustering analysis (Balslv et al., 2002; Fadili et al., 2000; Scarth and McIntyre, 1995). These methods emphasize the intrinsic structure of the data. An essential difference between these model-free approaches and SPM is that they are multivariate approaches accounting for interactions among different regions or voxels. The effects elicited by physiological or nonphysiological factors are extracted as 'spatial modes', for example, the principal components or eigenimages in PCA, or the center and the size of each cluster in clustering analysis. Among multivariate approaches, independent component analysis (ICA) has attracted attention recently and represents a promising approach to characterizing evoked responses (Calhoun et al., 2001a; McKeown et al., 1998a,b; Moritz et al., 2003; Sevensen et al., 2002). ICA is capable of extracting multiple sources such as task-related components, cardiac and respiratory effects, subject movements, and noise. The principal advantage, that almost all reports highlight, is its applicability to cognitive or motor control paradigms where detailed predictions of brain activity are not available, and no a priori information about the responses is available.

Nevertheless, there are limitations to purely data-driven approaches. It is difficult to put these approaches into a statistical framework that allows one to test the activations against a desired hypothesis. Furthermore, some basic assumptions of the ICA model, such as linear summation of the independent components, may not always be true across different datasets or different portions of the data. Finally, it lacks the ability to assess the local or regionally-specific nature of brain responses. An approach called 'HYBICA' has been proposed that allows one to use a priori hypotheses to guide the analysis (McKeown, 2000). This approach successively combines independent components to construct task-related components and then turns to a fully hypothesis-driven approach. We propose a similar if simpler approach that combines multivariate ICA with univariate SPM.

SPM is a fairly mature framework for neuroimaging data analysis and has been applied successfully in many situations. It would be nice to harness the inferential power of SPM to make inferences about data-led responses in a regionally-specific fashion. With an eye to this issue, we augmented SPM with model-free methods, namely ICA.

First, we describe briefly the theory of GLM and ICA to provide a background. More detailed treatments can be found in standard texts. After this, our approach to combining temporal ICA (tICA) and GLM is presented. In our approach, the design matrix of GLM is determined automatically using tICA decomposition. An fMRI study using our unified approach is then also presented. It should be noted that this method is not restricted to fMRI studies and can, in principle, be used for other types of studies such as optical imaging, PET, etc.

Materials and methods

Overview of the general linear model (GLM)

The GLM underlies most of the statistical analyses that are used in neuroimaging. It is the foundation for the t test, analysis of variance (ANOVA), analysis of covariance (ANCOVA), regression analysis, and many of the multivariate methods including factor analysis, cluster analysis, multidimensional scaling, discriminate function analysis, and canonical correlation. It is simply an equation that relates observations to expectations by expressing the observations (response variable) as a linear combination of expected components (or explanatory variables) and some residual error. Let x_i denote the observations, then the general linear model is:

$$x_i = g_{i1}\ \beta_1 + g_{i2}\ \beta_2 + \cdots + g_{ik}\ \beta_k + e_i \tag{1}$$

where $i = 1,\ldots,J$ is the index of observations, the coefficients g_{ik} are explanatory variables, and β_k are unknown parameters representing the weights of each of the explanatory variables. The model assumes that the errors e_i are independent and identically distributed normal random variables with zero mean and variance σ^2, written $e_i \overset{iid}{\sim} N(0, \sigma^2)$.

In SPM, the GLM used is as follows:

$$x_{ij} = g_{i1}\ \beta_{1j} + g_{i2}\ \beta_{2j} + \cdots + g_{ik}\ \beta_{kj} + e_{ij} \tag{2}$$

where x_{ij} denotes the response variable such as regional CBF at voxel $j = 1,\ldots,J$, i indexes scan, $e_{ij} \sim N(0, \sigma_j^2)$. The matrix form of Eq. (2) is:

$$\mathbf{X} = \mathbf{G}\beta + e \tag{3}$$

and can be regarded as a mass-univariate model.

The matrix $\mathbf{G}$ is called design matrix. It contains the explanatory variables relating to the specific experimental conditions under which the observations were made. They may be of direct interest (e.g., the effect of particular sensorimotor or cognitive condition, the degree of sensorimotor or cognitive processing, or the interaction of different factors). Others may pertain to confounding effects (e.g., the effect of being a particular subject, non-physiological noise due to instrument or head movement, physiological noise such as cardiac and respiratory effects). Each column of $\mathbf{G}$ is associated with an unknown parameter in vectors β_j.

Least squares estimates of β_{kj} are given uniquely by

$$\hat{\beta} = \left(\mathbf{G}^T\ \mathbf{G}\right)^{-1}\mathbf{G}^T\ \mathbf{X} \tag{4}$$

where $E\{\hat{\beta}_j\} = \beta_j$ and $\mathrm{Var}\{\hat{\beta}_j\} = \sigma_j^2\ (\mathbf{G}^T\ \mathbf{G})^{-1}$.

The residual variance can be estimated by the residual mean square,

$$\hat{\sigma}^2 = \frac{e^T e}{I-p} \sim \sigma^2\ \frac{\chi^2_{\ I-p}}{I-p} \tag{5}$$

where $p = \mathrm{rank}(G)$. The least squares estimates are themselves normally distributed, i.e., $\hat{\beta} \sim N(\beta,\ \sigma^2(G^TG)^{-1})$. For a column vector of J weights c, $c^T\hat{\beta} \sim N(c^T\beta, \sigma^2 c^T\ (G^TG)^{-1}c)$. Furthermore, $\hat{\beta}$ and $\hat{\sigma}^2$ are independent, thus pre-specified hypotheses concerning linear compounds of the model parameters can be assessed using

$$\frac{c^T\ \hat{\beta} - c^T\ \beta}{\sqrt{\hat{\sigma}^2\ c^T\ \left(\mathbf{G}^T\ \mathbf{G}\right)^{-1}c}} \sim t_{I-p} \tag{6}$$

That is, the hypothesis $H_0{:}c^T\beta = d$ can be assessed by comparing

$$T = \frac{c^T\ \hat{\beta} - d}{\sqrt{\hat{\sigma}^2\ c^T\ \left(\mathbf{G}^T\ \mathbf{G}\right)^{-1} c}}$$

with a Student's t distribution with $I - p$ degrees of freedom.

Overview of independent component analysis (ICA)

ICA has been used recently to characterize brain responses (Duann et al., 2002; Jung et al., 2001; Moritz et al., 2000). ICA attempts to separate independent 'sources' that have been mixed together (e.g., different speakers recorded on a single microphone, i.e., the 'cocktail party' problem).

Assume that n random variables $x_1,\ldots,x_n$ are observed and modeled as a linear combination of n random variables $s_1,\ldots,s_n$:

$$x_i = a_{i1}\ s_1 + a_{i2}\ s_2 + \cdots + a_{in}\ s_n \tag{7}$$

for all $i = 1,\ldots,n$, where $a_{ij}, i, j = 1,\ldots,n$ are some real coefficients. By definition, s_i $(i = 1,\ldots,n)$ are statistically independent. This is the basic ICA model, describing how the observations are generated by mixing the components s_i. Using the vector–matrix notation, Eq. (7) can be written as:

$$\mathbf{X} = \mathbf{AS} \tag{8}$$

The independent components s_i (abbreviated as ICs) are latent variables, meaning that they cannot be directly observed. Also the mixing coefficients a_{ij} are assumed to be unknown. We can only observe the random variables x_i, and must estimate a_{ij} and s_i using x_i.

The ICA model assumes (i) the ICs are statistically independent and (ii) they have non-Gaussian distributions. Under these assumptions, after estimating the matrix $\mathbf{A}$, we can compute its inverse $\mathbf{A}^{-1}$, and obtain the ICs simply with

$$\mathbf{S} = \mathbf{A}^{-1}\mathbf{X} \tag{9}$$

There are several methods to estimate $\mathbf{A}$ such as ICA by maximization of non-Gaussianity, by maximum likelihood estimation, by minimization of mutual information, and by tensorial methods, etc. (Hyvärinen et al., 2001).

Once ICA has been performed, we obtain the ICs and their mixing matrix. The ICs sometimes have some physical meaning. For example, in relation to the 'cocktail party' problem, each IC corresponds to one speaker, while the mixing matrix indicates the way in which their voices are mixed.

ICA, as applied to fMRI, can be used to separate either spatially (McKeown et al., 1998a) or temporally (Biswal and Ulmer, 1999; Makeig et al., 1997) independent sources. Suppose $\mathbf{X}$ is an N-by-M matrix (where N is the number of time points and M is the number of voxels in each scan and usually $N << M$). In spatial ICA (sICA), the signals are the M voxels and there are N different observations of these signals. Temporal ICA (tICA) considers the signals as N individual time courses of which there are M observations. At most M ICs can be obtained, each of which corresponds to a spatially independent component map (for sICA) or a temporally independent time course (for tICA).

A principal advantage of ICA is its applicability to paradigms in which detailed models of brain responses are not available (e.g., hallucinations and auditory analysis, see Seifritz et al., 2002). In these contexts, it is a more objective approach to the structure of the data than the model-based methods. However, ICA cannot establish the significance of each IC; the ICA model is not a statistical model that supports classical inference. This is because there is no null model to compare it with. Another way of looking at this is to note there is no observation error in the ICA model (Eq. (8)). Furthermore, the spatial characterization of treatment effects is in terms of spatial modes which have no regional specificity. In the following, we use SPM to make classical inferences about the region-specific expression of ICs obtained from tICA. This circumvents the two shortcoming of tICA, namely lack of inference and lack of regional specificity.

A unified method

Comparing Eq. (3) with Eq. (8), we note that the GLM and ICA models share common features. They both try to explain observations in terms of a linear combination of explanatory variables, which embody the structure of the observed data. The difference lies mainly in the causes of the data: the GLM uses hypothesis-led causes, whereas ICA is data-led. In the GLM, the number and the form of the explanatory variables are determined by a priori information and have explicit meaning or labels. It falls to the researcher to include all possible factors that may contribute to the data. Once the model is estimated, the un-modelled responses, whether meaningful or not, will be assigned to the error term. Conversely, in ICA, the dataset is decomposed into several explanatory variables that include all causes, irrespective of whether they were predicted or not. The problem now is that there are too many causes and there are no degrees of freedom left for making any inference about the interesting ones.

In the following, we introduce the notion of arbitrarily partitioning the ICs into signal and noise subspaces. This enables one to test the null hypothesis that the signal ICs contributed nothing to the data. Initially, this may seem rather circular because we already know the signal ICs are veridical causes of the data from the ICA. However, from the point of view of any single region, we have no idea whether these ICs were expressed or not. By adopting the mass-univariate approach of SPM, one can make regionally-specific inferences about the significance of the signal ICs that were obtained from the multivariate ICA. Clearly, this violates good statistical practice because we know a priori the null hypothesis is false. In other words, the tests will be slightly invalid with an increased false-positive rate. However, we will assume the contribution of any single region to the signal ICs will be sufficiently small to ignore this violation. We test this assumption using simulated data below.

In short, we will define a signal subspace on the basis of spatial distributed responses throughout the brain and then re-visit each voxel to see if these signals were expressed significantly in that region. This simple approach reduces to treating a subset of the ICs as potential explanatory variables that comprise the design matrix in the GLM. We then use established procedures (the theory of Gaussian random fields) to characterize significant regional responses with SPM.

There are three issues that need to be considered. The first is whether sICA or tICA is more appropriate for our purposes. This problem has been discussed elsewhere (Calhoun et al., 2001a; Stone et al., 2002). It has been suggested that when the basic assumptions of ICA hold true, i.e., the original causes are not strongly spatially or temporally dependent, a successful separation will be obtained. For the unified method, tICA is more appropriate than sICA

because ICs are time courses representing independent causes. This accords with the basic assumption of the GLM. Namely, that all voxels share the same explanatory variables. Furthermore, by enforcing independence among the temporal causes, there is a clear motivation for finding the regional correlates of these causes with SPM. sICA is predicated on assumptions about the spatial distribution of regional responses that are not embodied in the mass-univariate approach adopted by SPM.

It is noted that, tICA would not be viable if without an appropriate pre-processing procedure (Calhoun et al., 2001a). In practice, tICA is enabled by a dimension reduction prior to estimation of the mixing matrix. This is usually performed using principal component analysis (PCA) (Calhoun et al., 2001a; Makeig et al., 1997; Liu et al., 2004) to project the original dataset or reduced dataset with irrelevant voxels excluded on a new orthogonal coordinate system by maximizing the variance of the projected data. The first principal component corresponds to the direction with maximal variance, and the second expresses the greatest variance in the sub-space orthogonal to the first, and so on. Thus, the original dataset is decomposed into a small number of principal components that explain the most variance (energy) in the data. In summary, PCA can reduce the data dimension while preserving useful signals. This reduces the computational burden for tICA and increases the signal-to-noise ratio (SNR) (Hyvärinen et al., 2001).

Secondly, as mentioned above, ICA is a determinate model with no error term. However, degrees of freedom must be recovered to enable classical inference in the context of the GLM. This requires a bipartition of the ICs to define a small number of signal ICs that enter the design matrix, i.e., to determine the degrees of freedom of the model. Researchers have proposed several approaches model specification, for instance, the Bayesian information criterion (BIC) (Stoica and Selen, 2004; Thirion and Faugeras, 2003), Akaike information criterion (AIC) (Akaike, 1974), minimum description length (MDL) (Calhoun et al., 2001b; Rissanen, 1983; Thirion and Faugeras, 2003), deviance information criterion (DIC) (Woolrich et al., 2004). These criteria combine a goodness-of-fit measure (GOF) with a generalizability or complexity measure (number of parameters of the model, sample size, and functional form, etc.) so that the model is the best approximation to the underlying process, not simply the one that accounts for the most variation in the data (Pitt and Myung, 2002). In this sense, the BIC can be regarded as an approximation to the log of the model evidence (the probability of the data given a model).

We compute the BIC as follows:

$$\mathrm{BIC} = -2\ln(f(y \mid \theta_0)) + k\ln(M) \tag{10}$$

where y denotes the observed data, θ are the model parameters, θ_0 are the parameters that maximize the posterior probability density function $f(y|\theta)$, k is the number of parameters, M is the sample size. The model, with k parameters, that minimizes the criterion is chosen, when k corresponds to the number of ICs, constrained by the PCA dimension reduction. It is important to ensure that the PCA dimension reduction does not overly constrain the signal subspace; otherwise, the identification of 'independent' causes by ICA will be compromised.

Thirdly, one has to specify the ICs that constitute the signal subspace. In our work, we use those that show the greatest correlation with known experimental factors. This extends the marriage of data- and hypothesis-led approaches to another level. However, we note that the selection of signal ICs can be performed according to meaning of the inferences sought. For example, one could use ICs that expressed the greatest power at the fundamental frequency of designed experimental changes.

In summary, the unified method comprises the following steps: (i) dimension reduction with PCA, (ii) ICA using the BIC, to determine model order, (iii) use the temporal ICs to specify a design matrix for a GLM, and (iv) then use SPM to make inference about regional responses. The key contribution of the unified scheme is the marriage of ICA and SPM to endow data-led characterizations of brain responses with regional specificity. ICA is a multivariate approach that expresses independent responses in terms of spatial modes, which have no local or regional support. By borrowing devices from classical inference (namely random field theory) we are able to assess the significance of the expression of these modes at each point in the brain. This is achieved by testing the null hypothesis that the amount of variance explained by a subset of ICs is no greater than that explained by the remainder (assigned to a noise subspace). We can do this because the components are identified on the basis of their independence, not on the amount of variance they explain (this is in contradistinction to PCA).

Experimental design and data acquisition

Data were acquired in a GE Signa System operating at 1.5 T with a gradient echo EPI sequence (TR = 3.12 s, TE = 60 ms, FOV = 24 cm, matrix = 64 × 64, slice thickness = 5 mm, gap = 1.5 mm). Eight oblique slices were acquired, with an angle of approximately 20° to the AC–PC plane (Fig. 1). These slices were selected to cover the motor representation in the cortex, excluding the cerebellum and basal ganglion. Twelve healthy, right-handed subjects (six males and six females) were scanned while performing left hand and right hand movements. The movements were elicited with a periodic design consisting of 5 blocks of 20 scans. Each block consisted of 10 baseline scans followed by 10 scans of movement. The whole experiment lasted 312 s. Another null dataset was acquired from a healthy subject who performed no specific task.

Simulations and analysis

Monte Carlo simulations and analyses similar to those described by Della-Maggiore et al. (2002) were used to assess the power of the unified scheme. The null dataset was used for these simulations to provide realistic noise and endogenous variation in signal. Simulated activations were added to the null

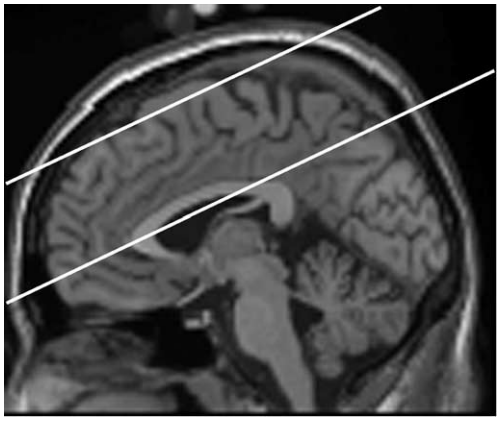

Fig. 1. Position of the two oblique slices providing coverage of the movement area in the cortex.

data at 50 randomly positioned regions. Each region consisted of 3 × 3 × 2 voxels (i.e., 11.25 × 11.25 × 10 mm). This process was repeated 10 times, resulting in 10 datasets with totally 500 'active' regions to evaluate the power.

We performed two groups of simulations with different forms of hemodynamic responses on the null dataset. For a parametric hemodynamic response, an HRF derived from Cohen (1997) was convolved with a four-period boxcar function. This signal was added to the baseline time-series of the 'active' regions. The HRF had the following form:

$$h(t) = t^{8.6}\ e^{(-t/0.547)} \tag{10}$$

where t is time. The magnitude was 1% of the average null signal amplitude.

For a nonparametric HRF, the response was constructed using the average response of the subjects making real movements. An SPM analysis (SPM2, Wellcome Department of Cognitive Neurology) was applied to the datasets of all subjects in the hand movement experiment (see next section). The mean time-series was calculated for each region that exhibited task-related changes. This was then normalized to lie between 0 and 1. This procedure gave 25 such time-series, some of which are shown in Fig. 2. For each of the 500 'active' regions, a randomly scaled time-series was added to the baseline. The magnitude of the added response was 2%, 3%, and 4%, respectively. The typical signal change in fMRI is between 2% and 4% for this paradigm.

The simulated data were analyzed using SPM and the unified method. For SPM, we used the conventional method to construct the design matrix. A boxcar stimulus function, convolved with a canonical HRF and its time derivate, was included. A set of 4 discrete cosine basis functions was appended to the design matrix to implement a high-pass filtering. This has been shown to increase the power of SPM (Della-Maggiore et al., 2002). For the unified method, tICA, based on Maximum Likelihood (ML, with $\tanh(\cdot)$ as the nonlinearity) algorithm, was applied to the time series, resulting in independent time courses (signal ICs) whose number was determined by the BIC. These ICs were sorted according to their correlation coefficients with the reference function and were entered into a design matrix. Parameters in the GLM were estimated where serial correlations were modeled with an AR(1) model. Statistical inference was performed under a series of alpha levels (t test, where the uncorrected P was varied from $1e^{-8}$ to 1). The status of each 'active' region was used to estimate sensitivity or power and as a function of the alpha-level (i.e., specificity).

Experimental data analysis

Left hand and right hand movement data for the 12 subjects were analyzed using the SPM2 software package. Spatial transformation (realignment, spatial normalization) was performed to correct for motion. Data were smoothed spatially with a Gaussian filter (4-mm full-width half-maximum (FWHM) kernel). The preprocessing is necessary for subsequent analysis and it has been verified that the smoothing does not change the ICA results markedly (this does not mean that smoothing does not affect ICA results in general, see Calhoun et al., 2001a). The other steps of model specification and parameters estimation were exactly the same as the simulation analysis. Statistical inferences were made about movement-related responses using the appropriate contrasts (t test, $P = 0.001$, uncorrected).

Results

Simulation results

The power of SPM and the SPM–ICA method were calculated, using simulated data, for different alpha levels and response amplitudes. The results shown in Fig. 3 indicate that under almost all the conditions, the unified method has higher power than SPM, which is evident especially when the hemodynamic response is nonparametric. The false-positive rates of the two methods are comparable under typical lower alpha levels, for example, $P = 0.001$. However, as expected, when the alpha value goes higher, the false-positive rate of the unified method is a little larger. The receiver operating characteristic (ROC) curves were used for further comparison (see Fig. 4). In most situations, the ROC curves of SPM–ICA are higher than those of SPM, which indicates that the unified method outperforms the conventional SPM.

The area under the ROC curve (AUC) was taken as a scalar measure (Hanley and McNeil, 1982). An area of 1 represents a perfect test; while 0.5 or below chance discrimination. When SNR was 1% for the nonparametric case, both SPM and the unified method failed to give good results (AUC = 0.4332, 0.4091). When SNR was 0.5% for the parametric case, SPM failed while SPM–ICA still works (AUC = 0.4691, 0.5593).

Results from the real datasets

Activations in the 12 subjects were similar, consistent, and replicable (Table 1). The areas corresponding to motor (premotor, sensorimotor and SMA) areas were identified. To highlight the difference between these two methods, we can apply logical 'OR' operation on the upper and lower part of Table 1 to obtain the number of occurrences of a region. For premotor and sensorimotor areas and SMA, both SPM and the unified method detected activations in all the 24 datasets. For temporal, frontal, cingulate, and parietal gyrus, the detected occurrence numbers of SPM versus the new method are 8/10, 7/11, 7/9, 10/12 for the left and

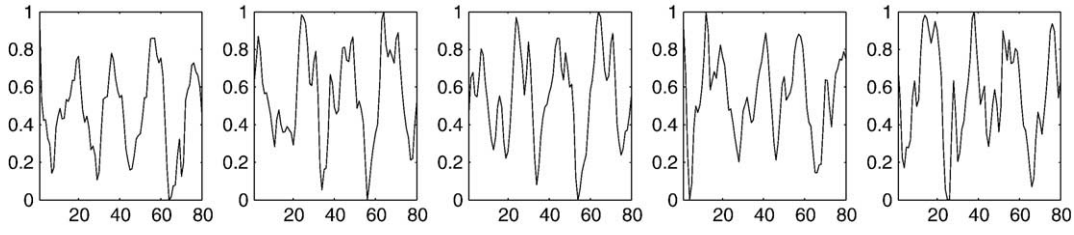

Fig. 2. Examples of hemodynamic responses extracted from the activation areas. These were added to the baseline signal to construct simulated data.

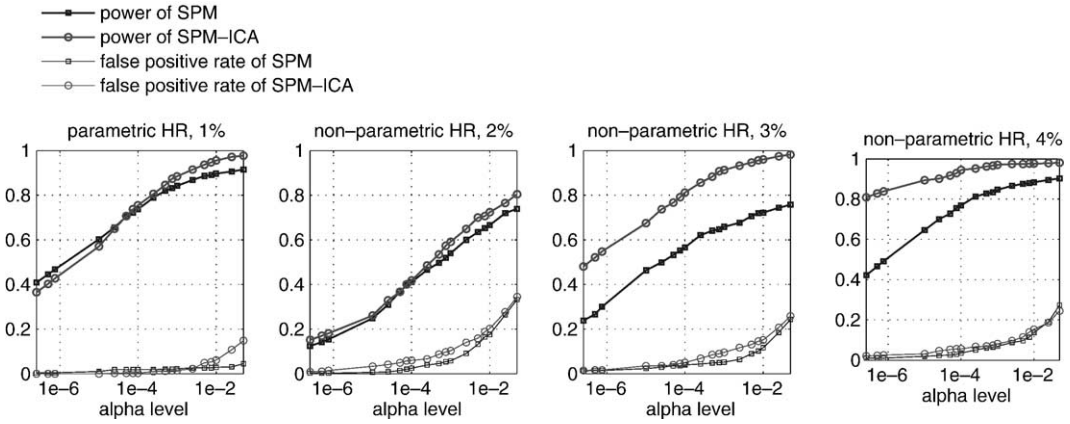

Fig. 3. Power analysis of the two methods. The baseline images were mixed with either a parametric or a nonparametric simulated response of differing magnitude. 1% means the magnitude of the hemodynamic response (HR) is 1% of the signal magnitude.

5/11, 10/12, 6/10, 9/12 for the right hand experiments, respectively. Thus, the SPM–ICA method has higher detection rates in this empirical analysis as suggested by the ROC analysis (Fig. 4).

To provide more detailed information, we present the results for subject 1 as an example (Figs. 5 and 6). The SPM results and the corresponding columns of design matrix are shown in Fig. 5. Similarly, results of the unified method are shown in Fig. 6.

The conventional SPM found some activation areas, e.g., the contralateral sensorimotor and premotor areas, supplementary motor areas, and ipsilateral premotor areas, in both left hand and right hand movement experiments (Figs. 5A and B). Allowing for slight onset differences, several parts of the parietal and inferior frontal regions were also activated (Figs. 5C and D). Comparing the results of our unified approach with those of the SPM method, we found similar activated areas (Figs. 6A and B). However, parts of the parietal and frontal cortex were found by our approach to be activated by both left and right hand movements, though differing in their relative positions (Figs. 6C and D). Some of these extra areas were also disclosed by conventional analyses when allowing for slight onset differences. However, more areas and more significant activations were found using the unified method.

Some activated areas showed responses that are consistently time-locked to the designed block called consistently task-related (CTR) components (McKeown et al., 1998a,b). Among the CTR areas, the bilateral premotor and sensorimotor areas and SMA appear to play a role in executing hand movement (Moritz et al., 2000, 2003; Umests et al., 2002). In addition, parts of the frontal, temporal, cingulate, and parietal gyrus also show the CTR characteristics. Specifically, the CTR time course rises at the onset of each stimulus, holds near the maximum value during the block, and decreases when the task is over. We found that only one component from each trial had a CTR time course closely matching the reference function (r = 0.9420 and 0.9052 for left and right hand movement, respectively, as shown in Figs. 6A and B).

It can be seen that the CTR curve is very similar to the HRF regressor. At the same time, the CTR component and HRF are not completely the same.

The temporal characteristics of the hemodynamic response, among different control-task blocks, are not exactly the same. The difference suggests that the subject's response is not always stable. In neuroimaging analysis, inference may be confounded by uncertainty due to a thing like warming-up of the machine, psychological and physiological preparation of the subject, etc. If we could anticipate or estimate such uncertainty during the design of model, the observed data could be modeled much better.

In contrast to the CTR areas, there were some transiently task-related (TTR) areas. The unified method shows that, though differences among subjects exist, parts of parietal and frontal cortex are TTR areas (Table 1 and Figs. 6C and D).

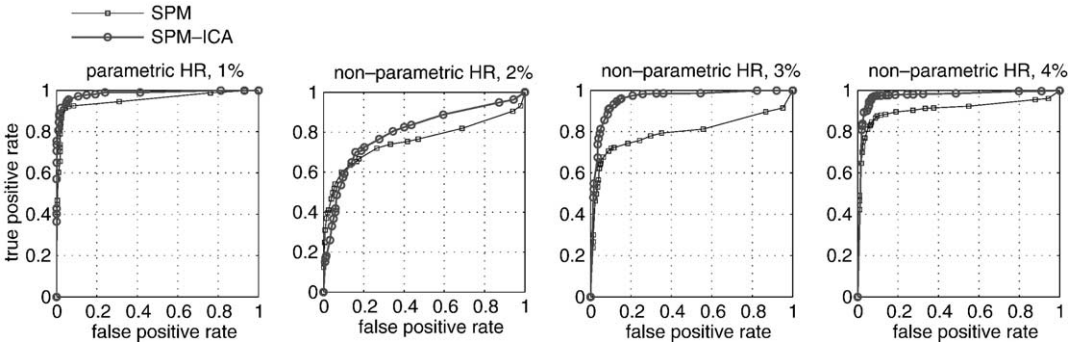

Fig. 4. The ROC curve of SPM and the unified method. The baseline images were mixed with either a parametric or nonparametric simulated response of differing magnitude. 1% means the magnitude of the hemodynamic response (HR) is 1% of the signal magnitude. For simulation with a parametric HR and 1% signal change, the area under the ROC curve (AUC) is 0.7668 and 0.7876 for SPM and SPM–ICA, respectively; for simulation with a nonparametric HR and 2% signal change, AUC = 0.5345 and 0.5427, respectively; for that with a nonparametric HR, 3% signal change, AUC = 0.6203 and 0.8241; and for a nonparametric HR, 4% signal change, AUC = 0.7708 and 0.9085.

Table 1
Individual subjects' activations for left and right hand movement experiments

	Anatomical structure	S 1		S 2		S 3		S 4		S 5		S 6		S 7		S 8		S 9		S 10		S 11		S 12		Total	
		L	R	L	R	L	R	L	R	L	R	L	R	L	R	L	R	L	R	L	R	L	R	L	R	L	R
HRF or CTR component predicted	Sensorimotor (C)	+/+	+/+	+/+	+/+	+/+	+/+	+/+	+/+	+/+	+/+	+/+	+/+	+/+	+/+	+/+	+/+	+/+	+/+	+/+	+/+	+/+	+/+	+/+	+/+	12/12	12/12
	Premotor (C)	+/+	+/+	+/+	+/+	+/+	+/+	+/+	+/+	+/+	+/+	+/+	+/+	+/+	+/+	+/+	+/+	+/+	+/+	+/+	+/+	+/+	+/+	+/+	+/+	12/12	12/12
	SMA (C)	+/+	+/+	+/+	+/+	+/+	+/+	+/+	+/+	+/+	+/+	+/+	+/+	+/+	+/+	+/+	+/+	+/+	+/+	+/+	+/+	+/+	+/+	+/	+/+	12/12	12/12
	Temporal (C)	+/+	−/−	+/+	+/+	+/+	−/+	+/+	−/+	+/+	−/+	−/+	−/+	−/+	−/+	−/+	−/+	−/+	−/+	−/+	−/+	−/+	−/−	+/+	−/+	6/10	2/10
	Sensorimotor (I)	+/+	+/+	+/+	+/+	+/+	−/−	+/+	−/−	+/+	−/+	+/+	−/+	−/+	−/+	+/+	+/+	−/+	+/+	−/+	+/+	−/+	−/−	+/+	−/+	9/12	6/10
	Premotor (I)	+/+	+/+	+/+	+/+	+/+	−/+	+/+	−/+	+/+	−/+	+/+	−/+	−/+	−/+	+/+	+/+	+/+	+/+	+/+	+/+	+/+	+/+	−/+	+/+	10/12	8/12
	SMA (I)	+/+	+/+	+/+	+/+	+/+	−/+	+/+	−/+	+/−	+/+	−/+	−/+	−/+	−/+	+/+	+/+	+/+	+/+	+/+	+/+	+/+	+/+	+/+	+/+	10/11	10/12
	Frontal	−/+	+/+	+/+	+/+	−/+	−/+	−/+	−/+	+/+	−/+	+/+	−/+	−/−	+/−	−/−	−/+	−/+	+/+	−/−	−/+	+/+	−/+	−/+	−/+	4/9	4/12
	CG	−/−	−/+	+/+	+/+	+/−	+/+	−/−	+/−	−/+	+/−	−/+	+/+	+/+	−/+	+/+	+/+	−/+	−/+	−/−	−/+	−/−	−/−	−/+	+/+	−/+	5/7	5/9
	Parietal	+/+	+/−	+/+	+/−	−/+	+/+	−/+	−/+	−/+	−/+	+/+	−/+	+/+	−/+	−/+	−/+	+/+	+/+	+/+	+/+	−/+	+/+	+/+	+/+	7/12	7/10
Temporal derivative of HRF or TTR component predicted	Sensorimotor (C)	−/+	+/−	−/−	+/−	+/−	−/−	+/−	+/−	+/−	+/−	+/−	+/−	+/−	+/−	+/−	+/−	−/−	+/+	−/−	−/+	+/+	+/+	−/+	+/+	8/3	8/6
	Premotor (C)	−/−	+/−	−/+	+/+	+/−	−/−	+/−	+/−	+/−	−/−	−/+	+/−	+/+	+/+	+/+	+/+	+/−	+/+	+/−	+/+	+/+	+/+	−/+	+/+	9/5	9/6
	Temporal (C)	−/−	−/−	−/−	−/−	−/−	−/−	+/+	−/−	+/−	−/−	+/−	+/−	+/−	+/−	+/+	−/−	+/−	−/−	−/+	−/−	−/−	−/−	−/+	+/+	−/+	−/−	5/2	3/3
	Frontal	−/+	−/+	−/+	−/+	−/+	−/+	−/+	+/+	+/−	+/−	+/+	−/−	−/+	+/+	−/+	+/+	+/−	+/+	+/−	+/−	+/−	+/−	+/−	−/+	5/8	8/7
	CG	−/+	−/−	−/−	+/+	+/−	+/+	−/+	+/+	+/−	+/−	+/+	−/−	−/+	−/+	−/+	+/+	−/−	+/+	−/−	−/−	−/−	−/−	−/−	+/+	4/6	6/6
	Parietal	+/+	+/+	+/+	−/+	+/+	+/+	−/+	+/+	−/−	−/−	+/+	−/−	−/+	+/+	+/+	+/+	−/−	+/+	−/−	−/+	+/−	−/−	−/+	−/+	6/8	5/9

Note. '+' indicates activations with significance of $P < 0.001$, uncorrected; '−' indicates absence of significant activation; activation results on the two sides of '/' are got by SPM and the unified method, respectively. Abbreviations used: S, subject; L, left hand movement; R, right hand movement; C, contralateral; I, ipsilateral; CG, cingulate gyrus.

TTR components have different temporal characteristics. There are several definitions of TTR, among which the most cited was posited by McKeown et al. (1998a,b). They defined TTR areas as those which are time-locked to the design during part of the task. They noted that some TTR components showed a marked activation at the onset of one or two of the task blocks, especially the early blocks, and suggested they may arise from shifts in performance strategy, from variations in subject arousal, attention, or effort, or from changes in brain activation produced by learning or habituation. Our results show that some TTR components (such as the curve in Fig. 6C) have this temporal characteristic. This can be seen in the first two blocks, where the time course is highly correlated with the CTR component. But in some paradigms, the TTR component is not the same. Their time courses may rise at the onset of each stimulus and then decrease quickly, forming a peak within each block, as can be seen in the curve in Fig. 6D. The regularity of these peaks may have some meaning. So we tried to extend the original definition of TTR by Mckeown et al. as follows: TTR components are those that are time-locked to the task-block design during part of the task or a part of the task block. Based on this definition, 19 TTR components were found in all 24 datasets (no obvious TTR components were found in the datasets of subject 5, right hand dataset of subject 6, and left hand datasets of subject 9 and subject 10, see Table 1). The physiological meaning of these TTR areas may relate to fast process concerned with information processing within the task, such as shifts of attention or effort as Mckeown et al. have pointed out, or even distraction from the task.

Anatomical and physiological evidence has demonstrated that the posterior parietal cortex may participate in motor preparation. It is also regarded as participating in somatosensory processing (Forss et al., 1997; Thees et al., 2003) and possibly sensorimotor integration (Mountcastle et al., 1975; Thees et al., 2003). An important function it performs is integrating the spatial relationship among objects through multimodal sensory input, and then linking this information with the position of the body. These computations are part of movement programming. It has also been demonstrated that the right part of the posterior parietal cortex is implicated in this function, which is consistent with our results, where the activated parietal areas locate mostly in the right hemisphere. Aside from the parietal cortex, activation was also found in the frontal cortex. Traditionally, the frontal lobe is thought to serve the function of planning, initiation, cessation, and evaluation of behavior. Mesial frontal cortex activation has been reported to contribute to both the preparation for movement and the descending activation of spinal motor networks (MacKinnon et al., 1996). Hence, from the functional attribution of these areas in the literature, it is not surprising that these areas showed TTR characteristics with an isolated peak near the onset of each stimulus.

Discussion

In this paper, we have described a combined data-led and hypothesis-led analysis procedure for fMRI time-series. In brief, after appropriate pre-processing, the multi-variate time-series are subject to ICA. The ensuing ICs over time are then used as explanatory variables in a general linear model to enable a conventional SPM analysis.

The SPMs are used to finesse the characterization of regionally specific brain responses in terms of a priori independent

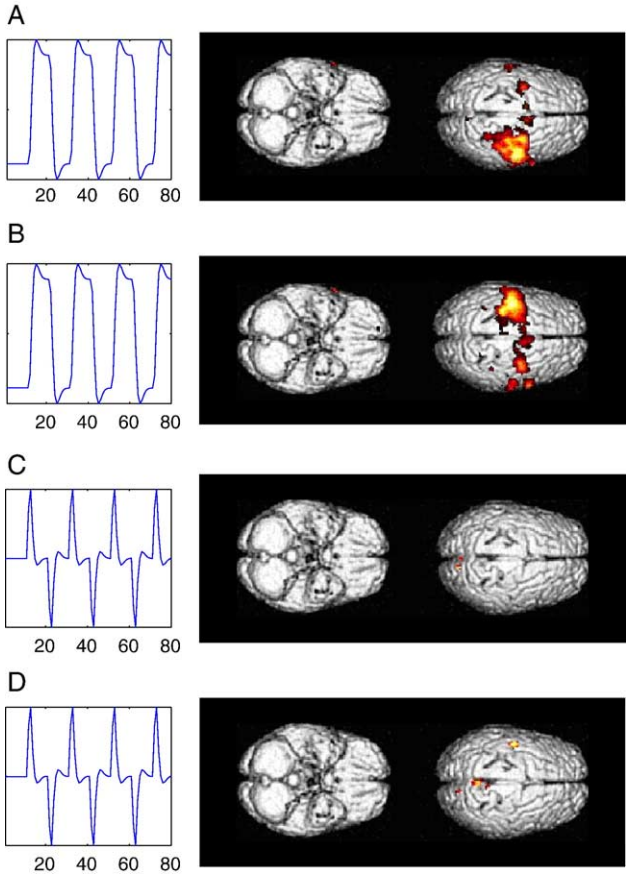

Fig. 5. Surface projection of subject 1's activated brain areas as detected by SPM. Panels A and C are results for left hand movement, and panels B and D are results for right hand movement. The corresponding columns of the design matrix are shown in the left of each panel.

component analysis. Critically, this rests upon a bipartition of the response variable into signal and noise. The signal lies in the space spanned by the ICs selected. The null space of these components contains noise. The SPM tests the variance lying in signal space against noise to disclose anatomically localized regions that have high signal to noise ratio.

Although our approach is not a valid classical inference procedure, it is interesting to reflect on the following argument: if we wanted to interpret the SPMs in terms of classical inference (i.e., declare the significant regionally specific responses), we would have to establish that the regressors or explanatory variables were formed independently of the data. One approach to this would be to derive the independent components from the left hand movement data and use them in a general linear model of the right hand movement data. However, this approach would not be sensitive to transiently task-related responses that were unique to either paradigm. An alternative argument is that omitting any single voxel or region from the independent component analysis would not affect the ensuing ICs to a great degree. If we assume that the ICs are the same with and without omitting a particular voxel, then the ICs can be regarded as being defined on the basis of independent data. In this case, the null hypothesis is that the voxel in question does not share any response profiles with the selected temporal modes or ICs used in the general linear model. This argument holds equally for all voxels and can be used as a partial motivation for interpreting the resulting SPMs in relation to a null hypothesis. Although this is an argument that deserves consideration, we reiterate that the SPM is used only to endow a regional specificity on brain responses given a signal-noise by-partition afforded by ICA.

Previously, we mentioned other model-free methods, such as PCA and clustering analysis. If ICAs were replaced by PCA in the unified method, there would be a fundamental problem, since the Type I error rate would be much higher than the established alpha level. This would make statistical inference extremely biased and invalid. ICA, in contradistinction to PCA, identifies the explanatory variables on the basis of their independence, not on the amount of variance they explain. Our simulations confirm that the Type I error rate of the unified method conforms to nominal levels when the alpha level is low (<0.01). This ensures that the use of SPM remains valid.

An issue that arises in practice is specifying the number of ICs. In our work, the number of ICs, according to the BIC criterion, varied between 4 and 12, with the mean value 8.17 and standard deviation 1.56. Thus, 12 ICs would have been sufficient to characterize our fMRI data. We have also performed the SPM–ICA analysis on all the real fMRI datasets with 12 ICs. The activation results were quite similar to those using SPM–ICA with the IC numbers selected by BIC.

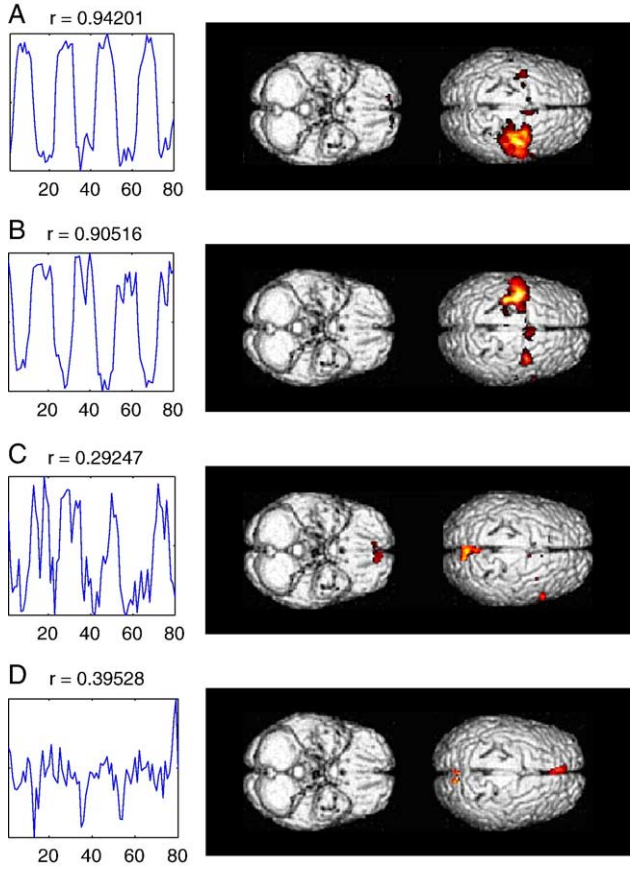

Fig. 6. Surface projection of subject 1's activated brain areas detected by the unified method. Panels A and C are results of left hand movement, and panels B and D are results of right hand movement. The design matrix was constructed using tICA. The curve in the left of the activation map is the corresponding column in the design matrix. Panels A and B indicate CTR components, and panels C and D TTR. Above each curve is its correlation coefficient with the reference function.

One may consider the stability of ICA decomposition in our scheme. From several tests, we found that the convergence is highly correlated with the cost function used by ICA and the dimension of the data. ICA by ML algorithm works well if we reduce the data dimension by PCA and exclude the irrelevant voxels successfully (Liu et al., 2004). More discussions about the convergence of ICA can be found in Hyvärinen et al. (2001).

Finally, in our experiment, the estimated ICs are sorted according to their correlation coefficients with the reference function. Some other methods such as power spectrum ranked ICA have been proposed (Moritz et al., 2003). The order of the ICs does not affect the estimation of parameters in GLM, but when making statistical inference the contrast of the variables should be carefully assigned. It is strongly recommended that, to supervise the decomposition procedure, indices related with correlation coefficients or power spectrum should be applied with proper threshold set in advance. Once the index is extremely low, it is well-founded that the corresponding components would not be so obviously related with the stimuli and could be excluded from the following statistical inference. If all the decomposed ICs have indices less than the threshold, then it is suggested that the dataset does not contain task-related components or the ICA decomposition fails with the current IC number. In our work, we have also performed the simulation on 0% signal level, which would inform directly on the type I error rate. The correlation coefficients of all ICs are less than 0.1. If statistical inference is carried on no matter what these indices are, the false-positive rate of SPM–ICA is obviously higher than that of SPM. But if we keep an eye on the indices, this kind of errors could be avoided.

Great attention has been paid by many research groups so far to ICA methods and their variants for fMRI. Our results demonstrated that the combination of SPM and ICA had some advantages.

SPM offers several options in model specification. These options make SPM flexible, but the choice of options is not always easy. Essentially, as a model-driven method, it has an inherent weakness: it does not extract the intrinsic structure of the data. If an accurate model of signal changes with respect to experimental events is not clear or constant across all voxels, this drawback is significant. To avoid mistakes, tests are required to estimate the accuracy of the specified model and some authors have made specific suggestions (Della-Maggiore et al., 2002; Strother et al., 2002). Using ICA for model specification requires only a little work. ICA decomposes the data according to the independence of the components instead of hypotheses about the data and can model not only useful signals, but also noise, which helps to construct a precise model of the data. Conventional methods, based on the assumption of the stationarity of brain responses, typically require averaging data over several task/control blocks. This makes them less sensitive to detecting TTR changes, although these may be of considerable interest (McKeown et al., 1998a,b). ICA can overcome this disadvantage. It can detect both CTR and TTR components. At the same time of detecting TTR areas, the CTR areas are characterized with greater precision. Intuitively, the activated areas around premotor and SMA together are separated by tICA (Figs. 5 and 6). Our method also augments the capability of ICA by putting it in the statistical framework supplied by SPM. A similar approach called ‘HYBICA’, which characterizes the fMRI data from spatial ICA and allows the researcher to construct a design matrix, has also been presented by McKeown (2000). Appropriate statistics can be computed on the resulting error terms after linear model fitting. However, using the simplest form of the GLM, which assumes that voxels are independent, ignoring intrinsic spatial and temporal autocorrelation of fMRI signals, the validity of the standard GLM statistical approach can be compromised (McKeown, 2000; Zarahn et al., 1997). Specifically, by considering task-related activity to be modeled as one static image and one task-related time course, HYBICA will inevitably miss some of the subtle transient changes caused by novelty or habituation. It is also noted that the popular correlation analysis can potentially be dangerous since the correlation coefficients between the transient task-related signals and the standard block design stimulus signals may not be large enough to reach the threshold set for defining the activation (McKeown, 2000).

Our unified method relies on temporal ICA, which has been used to disclose meaningful un-predicted and un-modelled dynamics in the auditory system (Seifritz et al., 2002). The ICs are time courses which correspond to the form of GLM. From this perspective, our new approach is presented from a more methodological perspective.

Moreover, the statistical criterion for the selection and validation of the tICA-based linear model is quite effective in solving the problem of under- or over- decomposition (in tICA more than sICA). HYBICA combines sequentially the ICs to compose CTR components, while the unified method identifies CTR components directly.

The premise that ICA can be correctly applied to neuroimaging data is based on the assumption that the ICA model is appropriate (Calhoun et al., 2001a; Hyvärinen et al., 2001). To date, this remains to be seen. Schemes to use the unified method to analyze multiple subjects need to be developed. ICA has already been extended for multi-subject analysis, referred to as Group ICA (see Calhoun et al., 2001b; Sevensen et al., 2002), and this will be of great interest in further development of the unified method.

Acknowledgments

The authors are grateful to the anonymous reviewers for their insightful comments, which certainly helped us to improve this work. The authors also thank Dr. Y.F. Zang in National Laboratory of Pattern Recognition of CAS, and Dr. B.C. Shan in Institute of High Energy Physics of CAS, for helpful comments on an earlier version of the manuscript. This work was partially supported by the Distinguished Young Scholars Fund of China (Grant 60225015), Natural Science Foundation of China (Grant 30370416, 60171003, 30100054), Ministry of Science and Technology of China (Grant 2001 CCA04100), Ministry of Education of China (TRAPOYT Project).

References

Adler, R.J., 1981. The geometry of random fields. John Wiley & Sons, Inc., New York.

Akaike, H., 1974. A new look at statistical model identification. IEEE Trans. Autom. Control 19, 716–723.

Backfrieder, W., 1996. Quantification of intensity variations in functional MR images using rotated principal components. Phys. Med. Biol. 41, 1425–1438.

Balslv, D., Nielsen, F.Å., Frutiger, S.A., Sidtis, J.J., Christiansen, T.B., Savarer, C., Strother, S.C., Rottenberg, D.A., Hansen, L.K., Paulson, O.B., Law, I., 2002. Cluster analysis of activity-time series in motor learning. Hum. Brain Mapp. 15, 135–145.

Biswal, B.B., Ulmer, J.L., 1999. Blind source separation of multiple signal sources of fMRI data sets using independent component analysis. J. Comput. Assist. Tomogr. 23, 265–271.

Calhoun, V.D., Adali, T., Pearlson, G.D., Pekar, J.J., 2001a. Spatial and temporal independent component analysis of functional MRI data containing a pair of task-related waveforms. Hum. Brain Mapp. 13, 43–53.

Calhoun, V.D., Adali, T., Pearlson, G.D., Pekar, J.J., 2001b. A method for making group inference from functional MRI data using independent component analysis. Hum. Brain Mapp. 14, 140–151.

Cohen, M.S., 1997. Parametric analysis of fMRI data using linear systems methods. NeuroImage 6, 93–103.

Della-Maggiore, V., Chau, W., Peres-Neto, P.R., McIntosh, A.R., 2002. An empirical comparison of SPM preprocessing parameters to the analysis of fMRI data. NeuroImage 17, 19–28.

Duann, J.R., Jung, T.P., Kuo, W.J., Yeh, T.C., Makeig, S., Hsieh, J.C., Sejnowski, T.J., 2002. Single-trial variability in event-related BOLD signals. NeuroImage 15, 823–835.

Fadili, M.J., Ruan, S., Bloyet, D., Mazoyer, B., 2000. A multistep unsupervised fuzzy clustering analysis of fMRI time series. Hum. Brain Mapp. 10, 160–178.

Forss, N., Merlet, I., Vanni, S., Hamalainen, M., Mauguiere, F., Hari, R., 1997. Activation of human mesial cortex during somatosensory target detection task. Brain Res. 734, 229–235.

Friston, K.J., Jezzard, P., Turner, R., 1994. Analysis of functional MRI time series. Hum. Brain Mapp. 1, 153–171.

Friston, K.J., Frith, C.D., Turner, R., Frackowiak, R.S., 1995a. Characterizing evoked hemodynamics with fMRI. NeuroImage 2, 157–165.

Friston, K.J., Holmes, A.P., Poline, J.B., Grasby, P.J., Williams, S.C., Frackowiak, R.S., Turner, R., 1995b. Analysis of fMRI time-series revisited. NeuroImage 2, 45–53.

Friston, K.J., Holmes, A.P., Worsley, K., Poline, J.B., Frith, C., Frackowiak, R.S.J., 1995c. Statistical parametric maps in functional imaging: a general linear approach. Hum. Brain Mapp. 2, 189–210.

Friston, K.J., Fletcher, P., Josephs, O., Holmes, A., Rugg, M.D., Turner, R., 1998. Event-related fMRI: characterizing differential responses. NeuroImage 7, 30–40.

Grinvald, A., Slovin, H., Vanzetta, I., 2000. Non-invasive visualization of cortical columns by fMRI. Nat. Neurosci. 3, 105–107.

Hanley, J.A., McNeil, B.J., 1982. The meaning and use of the area under a receiver operating characteristic (ROC) curve. Radiology 143, 2936.

Hyvärinen, A., Karhunen, J., Oja, E., 2001. Independent component analysis, first ed. John Wiley and Sons, Inc., New York.

Jung, T.P., Makeig, S., McKeown, M.J., Bell, A.J., Lee, T.W., Sejnowski, T.J., 2001. Imaging brain dynamics using independent component analysis. Proc. IEEE 89, 1107–1122.

Lindauer, U., Royl, G., Leithner, C., Kuhl, M., Gold, L., Gethmann, J., Kohl-Bareis, M., Villringer, A., Dirnagl, U., 2001. No evidence for early decrease in blood oxygenation in rat whisker cortex in response to functional activation. NeuroImage 13, 988–1001.

Liu, Y., Zhou, Z., Hu, D., Yan, L., Tan, C., Wu, D., Yao, S., 2004. A novel method for spatio-temporal pattern analysis of brain fMRI data. Sci. China 34, 1139–1147.

MacKinnon, C.D., Kapur, S., Hussey, D., Verrier, M.C., Houle, S., Tatton, W.G., 1996. Contributions of the mesial frontal cortex to the premovement potentials associated with intermittent hand movements in humans. Hum. Brain Mapp. 4, 1–22.

Makeig, S., Jung, T.P., Bell, A.J., Ghahremani, D., Sejnowski, T.J., 1997. Blind separation of auditory event-related brain responses into independent components. Proc. Natl. Acad. Sci. U. S. A. 94, 10979–10984.

Mayhew, J., 2003. A measured look at neuronal oxygen consumption. Science 299, 1023–1024.

Mayhew, J., Hu, D., Zheng, Y., Askew, S., Hou, Y., Berwick, J., Coffey, P., Brown, N., 1998. An evaluation of linear model analysis techniques for processing images of microcirculation activity. NeuroImage 7, 49–71.

Mayhew, J., Zheng, Y., Hou, Y., Vuksanovic, B., Berwick, J., Askew, S., Coffey, P., 1999. Spectroscopic analysis of changes in remitted illumination: the response to increased neural activity in brain. NeuroImage 10, 304–326.

Mayhew, J., Hohnston, D., Martindale, J., Jones, M., Berwick, J., Ying, Z., 2001. Increased oxygen consumption following activation of brain: footnotes using spectroscopic analysis of neural activity in barrel cortex. NeuroImage 13, 975–987.

McKeown, M.J., 2000. Detection of consistently task-related activations in fMRI data with hybrid independent component analysis. NeuroImage 11, 24–35.

McKeown, M.J., Jung, T.P., Makeig, S., Brown, G., Kindermann, S.S., Lee, T.W., Sejnowski, T.J., 1998a. Spatially independent activity patterns in functional MRI data during the stroop color-naming task. Proc. Natl. Acad. Sci. U. S. A. 95, 803–810.

McKeown, M.J., Makeig, S., Brown, G.G., Jung, T.P., Kindermann, S.S., Bell, A.J., Sejnowski, T.J., 1998b. Analysis of fMRI data by blind separation into independent spatial components. Hum. Brain Mapp. 6, 160–188.

Moritz, C.H., Haughton, V.M., Cordes, D., Quigley, M., Meyerand, M.E., 2000. Whole-brain functional MR imaging activation from a finger-tapping task examined with independent component analysis. AJNR Am. J. Neuroradiol. 21, 1629–1635.

Moritz, C.H., Rogers, B.P., Meyerand, M.E., 2003. Power spectrum ranked independent component analysis of a periodic fMRI complex motor paradigm. Hum. Brain Mapp. 18, 111–122.

Mountcastle, V.B., Lynch, J.C., Georgopoulos, A., Sakata, H., Acuna, C., 1975. Posterior parietal association cortex of the monkey: command functions for operations within extrapersonal space. J. Neurophysiol. 38, 871–908.

Pitt, M.A., Myung, I.J., 2002. When a good fit can be bad. Trends Cogn. Sci. 6 (10), 421–425.

Rissanen, J., 1983. A universal prior for integers and estimation by minimum description length. Ann. Stat. 11, 416–431.

Scarth, G., McIntyre, M., 1995. Detection of novelty in functional images using fuzzy clustering. Proc. ISMRM 95 Nice 1, 238.

Seifritz, S., Esposito, F., Hennel, F., Mustovic, H., Neuhoff, J.G., Bilecen, D., Tedeschi, G., Scheffler, K., Salle, F.D., 2002. Spatiotemporal pattern of neural processing in the human auditory cortex. Science 297, 1706–1708.

Sevensen, M., Kruggel, F., Benali, H., 2002. ICA of fMRI group study data. NeuroImage 16, 551–563.

Stoica, P., Selen, Y., 2004. Model-order selection. IEEE Signal Process. Mag. 21 (4), 36–47.

Stone, J.V., 2001. Blind source separation using temporal predictability. Neural Comput. 13, 1559–1574.

Stone, J.V., Porrill, J., Porter, N.R., Willkinson, I.D., 2002. Spatiotemporal independent component analysis of event-related fMRI data using skewed probability density functions. NeuroImage 15, 407–421.

Strother, S.C., Anderso, J., Hansen, L.K., Kjems, U., Kustra, R., Sidtis, J., Frutiger, S., Muley, S., LaConte, S., Rottenberg, D., 2002. The quantitative evaluation of functional neuroimaging experiments: the NPAIRS data analysis framework. NeuroImage 15, 747–771.

Thees, S., Blankenburg, F., Taskin, B., Curio, G., Villringer, A., 2003. Dipole source localization and fMRI of simultaneously recorded data applied to somatosensory categorization. NeuroImage 18, 707–719.

Thirion, B., Faugeras, O., 2003. Dynamical components analysis of fMRI data through kernel PCA. NeuroImage 20, 34–49.

Thompson, J.K., Peterson, M.R., Freeman, R.D, 2003. Single-neuron activity and tissue oxygenation in the cerebral cortex. Science 299, 1070–1072.

Umests, A., Okuda, J., Fujii, T., Tsukiura, T., Nagasaka, T., Yanagawa, I., Sugiura, M., Inoue, K., Kawashima, R., Suzuki, K., Tabuchi, M., Murata, T., Mugikura, S., Higano, S., Takahashi, S., Fukuda, H., Yamadori, A., 2002. Brain activation during the fist-edge-palm test: a functional MRI study. NeuroImage 17, 385–392.

Woolrich, M.W., Jenkinson, M., Brady, J.M., Smith, S.M., 2004. Fully Bayesian spatio-temporal modeling for fMRI data. IEEE Trans. Med. Imag. 23 (2), 213–231.

Zarahn, E., Aguirre, G.K., D'Esposito, M., 1997. Empirical analyses of BOLD fMRI statistics: I. Spatially unsmoothed data collected under null-hypothesis conditions. NeuroImage 5, 179–197.